 SL, vol.4, no.1, pp.1-10, 2010

Determination of Interior Point Solutions for 3D Generally Anisotropic Elastic Solids by the Boundary Element Method

C. L. Tan[1] **and Y.C. Shiah**[2]

Abstract: Using newly derived explicit algebraic forms of the first- and second-order derivatives of the Green's function, interior point solutions for the displacements and stresses in 3D generally anisotropic elastic bodies are obtained using the boundary element method (BEM). The approach, which follows the same vein as in BEM for isotropic elasticity via Somigliana's identities, has not been successfully achieved previously in the literature due to the analytical difficulties involved with using the non-explicit forms of the Green's function. The veracity of the formulation and implementation is demonstrated by some examples.

Keywords: Anisotropic elasticity, Stroh's eigenvalues, boundary element method, Somigliana's identity.

1 Introduction

In the boundary element method (BEM), interior point solutions for the displacements and the stresses at an interior point of an elastic body are obtained from the numerical evaluation of the Somigliana's identities. It is carried out as a secondary exercise in the BEM analysis, after the boundary integral equation (BIE) has been solved for all the unknown displacements and tractions on the surface of the domain. In the integrals of these identities, the integrands contain terms with up to second- order derivatives of the Green's function for the displacements of the elastic problem. Although the BEM is a boundary solution technique, the displacements and stresses at interior points of the solid are sometimes required, e.g., for calculating J- or M-integrals in fracture mechanics analysis.

The Green's function, or fundamental solution, for displacements and that for tractions are necessary items for the direct formulation of the BEM for elastic stress analysis. For 3D generally anisotropic solids, Lifschitz and Rozentsweig (1947)

[1] Dept. of Mechanical & Aerospace Engineering, Carleton University, Ottawa, Canada K1S 5B6
[2] Dept. of Aerospace and Systems Engineering, FengChia University, Taichung, Taiwan R.O.C.

have presented the Green's function for displacements in 1947. The numerical evaluation of these fundamental solutions has remained a subject of investigation over the past few decades in the development of the BEM to treat such bodies; see, e.g. Wilson and Cruse (1978); Sales and Gray (1998); Tonon *et al* (2001); Phan *et al* (2004); Wang and Denda (2007); Tan *et al* (2009). This is because of their mathematical complexity. In the BEM formulation presented by the present authors recently, Tan *et al* (2009), the fundamental solutions employed in the BIE are expressed in algebraic, real-variable explicit forms, unlike those used previously by the other authors. They were derived by Ting and Lee (1997) for displacements, and Lee (2003) for their first derivatives, respectively; the latter being utilized for the derivation of the traction solution. These Green's functions were used for the first time in a BEM formulation. Because of their algebraic forms, they can be numerically evaluated in a fairly straightforward manner. Their implementation into an existing BEM code which had been developed for 3D isotropic elastostatics was also carried out without any difficulty. It was, however, discovered that a significant proportion of the computational effort is spent on evaluating high-order tensor terms which appear in Lee's (2003) solution. Lee (2009) re-examined her solution and showed how the first derivatives of the displacement Green's function can be obtained without introducing the high-order tensors. This is achieved by carrying out the partial differentiation in a spherical coordinate system as an intermediate step; the explicit expressions are, however, presented only for the special case of transverse isotropy in (2009). Following this development, the present authors derived the corresponding fully explicit forms of the solution for the displacement first derivatives in general anisotropy. Their validity and superior efficiency of using these alternative fully explicit forms of the fundamental solutions in the BIE is demonstrated very recently in Shiah *et al* (2008).

Of significance to note too about Lee's (2009) revised approach is that it also lends itself more readily to obtaining higher order derivatives of the Green's function for the displacements, again without the need to introduce high-order tensor quantities. The present authors have further derived the expressions, in fully explicit algebraic forms, of the second derivatives of the displacement fundamental solution Shiah *el al* (2011). This enables the implementation of the BEM to obtain the displacements and stresses at an interior point of a 3D generally anisotropic solid as well; it is the focus of the present paper. To the authors' knowledge, this development has never been reported previously in the literature. Some examples are presented in which the numerical solutions obtained are compared with those obtained using the FEM to demonstrate their validity.

2 The BEM for 3D Anisotropic Elasticity

In BEM for linear elasticity, the boundary integral equation (BIE) is an integral constraint equation relating displacements, u_i, to the tractions, t_i, on the surface of the domain. It may be written as follows,

$$C_{ij}u_i(P)+\int_S u_i(Q)T_{ij}(P,Q)dS=\int_S t_i(Q)U_{ij}(P,Q)dS+\int_\Omega X_i(q)U_{ij}(P,q)d\Omega \quad (1)$$

where the leading coefficient $C_{ij}(P)$ depends upon the local geometry of S at the source point P; $U_{ij}(P,Q)\equiv \mathbf{U}$, and $T_{ij}(P,Q)$ represent, the fundamental solutions of displacements and tractions, respectively, in the x_i-direction at the field point Q due to a unit load in the x_j-direction at P in a homogeneous infinite body. Once eq. (1) has been solved for all the unknown displacements and tractions on the surface S of the solution domain, the displacement at an interior point p of the body can be determined from Somigliana's identity, viz,

$$C_{ij}u_i(P)+\int_S u_i(Q)T_{ij}(P,Q)dS=\int_S t_i(Q)U_{ij}(P,Q)dS+\int_\Omega X_i(q)U_{ij}(P,q)d\Omega \quad (2)$$

The corresponding stresses may be obtained using the generalized Hooke's law:

$$\sigma_{ij}=C_{ijmn}\left(u_{m,n}+u_{n,m}\right)/2 \quad (3)$$

In eq. (3), the 1^{st}-order derivatives of displacements are obtained by differentiating eq. (2), viz.

$$C_{ij}u_i(P)+\int_S u_i(Q)T_{ij}(P,Q)dS=\int_S t_i(Q)U_{ij}(P,Q)dS+\int_\Omega X_i(q)U_{ij}(P,q)d\Omega \quad (4)$$

The Green's function $\mathbf{U}$ employed here is that derived by Ting and Lee (1997), which can be expressed in simple closed-form as

$$\mathrm{U}(\mathbf{x})=\frac{1}{4\pi r}\mathbf{H}[\mathbf{x}]=\frac{1}{|\mathbf{T}|}\sum_{\mathrm{n}=0}^{4}\mathrm{q_n}\hat{\boldsymbol{\Gamma}}^{(\mathrm{n})} \quad (5)$$

where r is the radial distance between the load and field point, and, **H[x]**, is the Barnett-Lothe tensor. The expressions for$|\mathbf{T}|$, $\hat{\boldsymbol{\Gamma}}^{(\mathrm{n})}$ and $\mathrm{q_n}$ in eq. (5) may be found in [7, 8]. The numerical evaluation of T_{ij} that is required in eq. (1) and eq. (2) may be carried out using the relationship between tractions and stresses, and the generalized Hooke's law, namely,

$$T_{ij}=\sigma_{ik}^{(j)}N_k, \quad (6)$$

$$\sigma_{ik}^{(j)} = C_{ikmn}\left(U_{mj,n} + U_{nj,m}\right)/2 \tag{7}$$

In eq. (6), $\sigma_{ik}^{(j)}$ are the stresses at a field point due to a unit concentrated force applied in the x_j direction at the source point, and N_k are components of the outward normal vector of the surface at Q. From the above, it is clear that the 1^{st}-order derivatives of **U** must first be obtained in order to evaluate the fundamental solution for stresses or tractions. Also, from eqs.(4)–(6), the second order derivatives of **U** are required as well.

Instead of carrying out the differentiation of the Green's function directly in the Cartesian coordinate system, the partial derivatives can be obtained in a spherical coordinate system as an intermediate step and the chain rule then employed, as follows

$$U_{ij,l} = \frac{\partial U_{ij}}{\partial r}\frac{\partial r}{\partial x_l} + \frac{\partial U_{ij}}{\partial \theta}\frac{\partial \theta}{\partial x_l} + \frac{\partial U_{ij}}{\partial \phi}\frac{\partial \phi}{\partial x_l} \tag{8}$$

$$U_{ij,kl} = \frac{\partial U_{ij,k}}{\partial r}\frac{\partial r}{\partial x_l} + \frac{\partial U_{ij,k}}{\partial \theta}\frac{\partial \theta}{\partial x_l} + \frac{\partial U_{ij,k}}{\partial \phi}\frac{\partial \phi}{\partial x_l} \tag{9}$$

In doing so, Lee (2009) shows that no high order tensor quantities need to be introduced. The partial derivatives above can be shown to be expressed as:

$$\frac{\partial U_{ij}}{\partial r} = \frac{-U_{ij}}{r}, \quad \frac{\partial U_{ij}}{\partial \theta} = \frac{I'_{ij} - J'_{ij}}{4\pi^2 r}, \quad \frac{\partial U_{ij}}{\partial \varphi} = \frac{I''_{ij} - J''_{ij}}{4\pi^2 r} \tag{10}$$

$$\begin{aligned}\frac{\partial U_{ij,k}}{\partial r} = {} & \frac{\partial^2 U_{ij}}{\partial r^2}\frac{\partial r}{\partial x_k} + \frac{\partial U_{ij}}{\partial r}\frac{\partial}{\partial r}\left(\frac{\partial r}{\partial x_k}\right) \\ & + \frac{\partial^2 U_{ij}}{\partial r \partial \theta}\frac{\partial \theta}{\partial x_k} + \frac{\partial U_{ij}}{\partial \theta}\frac{\partial}{\partial r}\left(\frac{\partial \theta}{\partial x_k}\right) + \frac{\partial^2 U_{ij}}{\partial r \partial \varphi}\frac{\partial \varphi}{\partial x_k} + \frac{\partial U_{ij}}{\partial \varphi}\frac{\partial}{\partial r}\left(\frac{\partial \varphi}{\partial x_k}\right),\end{aligned}$$

$$\begin{aligned}\frac{\partial U_{ij,k}}{\partial \theta} = {} & \frac{\partial^2 U_{ij}}{\partial r \partial \theta}\frac{\partial r}{\partial x_k} + \frac{\partial U_{ij}}{\partial r}\frac{\partial}{\partial \theta}\left(\frac{\partial r}{\partial x_k}\right) \\ & + \frac{\partial^2 U_{ij}}{\partial \theta^2}\frac{\partial \theta}{\partial x_k} + \frac{\partial U_{ij}}{\partial \theta}\frac{\partial}{\partial \theta}\left(\frac{\partial \theta}{\partial x_k}\right) + \frac{\partial^2 U_{ij}}{\partial \theta \partial \varphi}\frac{\partial \varphi}{\partial x_k} + \frac{\partial U_{ij}}{\partial \varphi}\frac{\partial}{\partial \theta}\left(\frac{\partial \varphi}{\partial x_k}\right),\end{aligned}$$

$$\begin{aligned}\frac{\partial U_{ij,k}}{\partial \varphi} = {} & \frac{\partial^2 U_{ij}}{\partial r \partial \varphi}\frac{\partial r}{\partial x_k} + \frac{\partial U_{ij}}{\partial r}\frac{\partial}{\partial \varphi}\left(\frac{\partial r}{\partial x_k}\right) \\ & + \frac{\partial^2 U_{ij}}{\partial \theta \partial \varphi}\frac{\partial \theta}{\partial x_k} + \frac{\partial U_{ij}}{\partial \theta}\frac{\partial}{\partial \varphi}\left(\frac{\partial \theta}{\partial x_k}\right) + \frac{\partial^2 U_{ij}}{\partial \varphi^2}\frac{\partial \varphi}{\partial x_k} + \frac{\partial U_{ij}}{\partial \varphi}\frac{\partial}{\partial \varphi}\left(\frac{\partial \varphi}{\partial x_k}\right)\end{aligned}$$

$$\frac{\partial^2 U_{ij}}{\partial r^2} = \frac{U_{ij}}{r^2} - \frac{\partial U_{ij}}{\partial r}, \quad \frac{\partial^2 U_{ij}}{\partial r \partial \theta} = -\frac{1}{r^2}\frac{\partial U_{ij}}{\partial \theta}, \quad \frac{\partial^2 U_{ij}}{\partial r \partial \phi} = -\frac{1}{r^2}\frac{\partial U_{ij}}{\partial \phi}$$

$$\frac{\partial^2 U_{ij}}{\partial \theta^2} = \frac{1}{4\pi^2 r}\left(\frac{\partial I'_{ij}}{\partial \theta} - \frac{\partial J'_{ij}}{\partial \theta}\right),$$

$$\frac{\partial^2 U_{ij}}{\partial \varphi^2} = \frac{1}{4\pi^2 r}\left(\frac{\partial I''_{ij}}{\partial \varphi} - \frac{\partial J''_{ij}}{\partial \varphi}\right), \frac{\partial^2 U_{ij}}{\partial \theta \partial \varphi} = \frac{1}{4\pi^2 r}\left(\frac{\partial I''_{ij}}{\partial \theta} - \frac{\partial J''_{ij}}{\partial \theta}\right) \tag{11}$$

In eqs.(10)-(12), I'_{ij}, I''_{ij}, J'_{ij}, J''_{ij} can be reduced to relatively direct, algebraic expressions in terms of the Stroh's eigenvalues. The explicit algebraic expressions for the component terms of $U_{ij,l}$ and $U_{ij,kl}$ above have been derived very recently by the present authors Shiah *el al* (2011). As they are fairly elaborate, they will not be presented here because of space limitations.

3 Numerical Results

Two examples are presented below to demonstrate the veracity of the BEM formulation developed for obtaining the displacements and stresses at an interior point of a generally anisotropic solid. The BEM solutions for the surface points of these two problems have been obtained and discussed in a previous study [7]; the focus here is on the solutions for the interior points only.

Example (A): The first example is a rectangular alumina (Al_2O_3) crystal prism subjected to a uniform shear stress $\tau_{23}= \tau_o= 1$ on four of its sides, as shown in Fig. 1(a). The exact analytical solution for the displacements in the body of this problem can be found in Lekhnitskii (1963). For the purpose of illustration, the displacements and all the stress components are obtained for five arbitrarily selected points inside the prism. The stiffness coefficients for the Al_2O_3 crystal are taken to be as follows Huntington (1968):

C_{11}= 465 GPa; C_{33}= 563 GPa; C_{44}= 233 GPa; C_{12}= 124 GPa;

C_{13}= 117 GPa; C_{14}= 101 GPa.

All the elastic stiffness coefficients defined are arranged in accordance with the generalized stress/strain relation:

$$(\sigma_{11}\ \sigma_{22}\ \sigma_{33}\ \sigma_{23}\ \sigma_{13}\ \sigma_{12})^T = \mathbf{C}\ (\varepsilon_{11}\ \varepsilon_{22}\ \varepsilon_{33}\ \gamma_{23}\ \gamma_{13}\ \gamma_{12})^T. \tag{12}$$

Figure 1(b) shows the BEM mesh employed; it has 10 quadratic boundary elements with a total of 32 nodes. The comparison of all the BEM-computed displacements and stresses with analytical solutions for the sample internal points is shown in Table 1. The agreement of the two corresponding sets of results can be seen to be excellent.

Table 1: Displacements and stresses at internal points – *Example (A)*.

	Int. point coord.	(0, 0.5, 0.5)	(0, 0.25, 0.5)	(0, 0, 0.5)	(0, -0.25, 0.5)	(0, -0.5, 0.5)
u_1	BEM	-0.4E-09	-0.8E-09	-0.7E-0	-0.1E-09	0.8E-09
	Exact	0	0	0	0	0
u_2	BEM	0.85522E-03	0.42762E-03	0.19500E-07	-0.42758E-03	-0.85518E-03
	Exact	0.85519E-03	0.42760E-03	0	-0.42760E-03	-0.85519E-03
u_3	BEM	0.28874E-02	0.14437E-02	0.17400E-07	-0.14437E-02	-0.28874E-02
	Exact	0.28873E-02	0.14437E-02	0	-0.14437E-02	-0.28873E-02
σ_{11}	BEM	-0.61539E-05	-0.34317E-05	-0.49309E-05	-0.25667E-05	-0.47013E-05
	Exact	0	0	0	0	0
σ_{22}	BEM	0.34529E-05	0.38731E-05	0.42609E-05	0.48083E-05	0.41356E-05
	Exact	0	0	0	0	0
σ_{33}	BEM	-0.16045E-05	-0.8133E-06	-0.7556E-06	-0.23678E-05	-0.13421E-05
	Exact	0	0	0	0	0
σ_{12}	BEM	-0.39420E-06	0.11470E-06	-0.10000E-06	-0.18560E-06	0.27940E-06
	Exact	0	0	0	0	0
σ_{23}	BEM	1.00000	1.00000	0.999998	1.000000	1.00000
	Exact	1	1	1	1	1
σ_{13}	BEM	-0.15336E-05	-0.82960E-06	-0.66590E-06	-0.49110E-06	0.10180E-06
	Exact	0	0	0	0	0

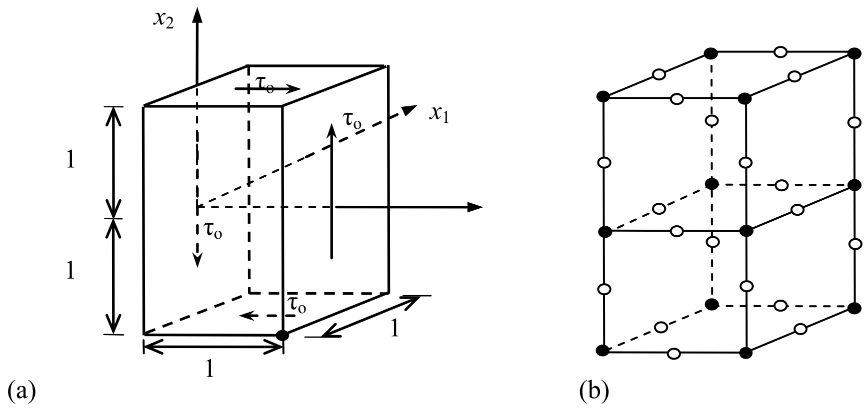

Figure 1: (a) A rectangular prism under uniform shear stress - *Example (A)*; (b) BEM mesh: 10 elements, 32 nodes.

Example (B): The second example is a cylindrical bar with a spherical cavity (see Fig. 3a), fixed at one end and subjected to a uniform unit tensile load at the other end. The case considered is for a/R = 0.4, H/R = 2. The resultant normalized displacements and the normalized von Mises equivalent stress, σ_{eq}/σ_o, at a series of points around the circle at radius $r = 0.75R$ are obtained here. The material is taken to be a niobium (*Nb*) crystal, a cubic material with the elastic stiffness constants (Huntington (1968)): C^*_{11}= 246 GPa; C^*_{12}= 134 GPa; C^*_{44}= 28.7 GPa, where the asterisks denote properties defined in the directions of the material principal axes. For the analysis, these axes are deliberately rotated successively about the x_1-axis, x_2-axis, and x_3-axis counterclockwise by 15^o, 30^o, and 45^o, respectively, which yields the following fully populated stiffness matrix:

$$\mathbf{C} = \begin{pmatrix} 218.76 & 153.52 & 141.72 & -10.01 & 0.40 & 7.21 \\ 153.52 & 209.89 & 150.59 & -2.21 & 0.96 & -0.18 \\ 141.72 & 150.59 & 221.69 & 12.22 & -1.36 & -7.04 \\ -10.01 & -2.21 & 12.22 & 45.29 & -7.04 & 0.96 \\ 0.40 & & 0.96 & -1.36 & -7.0436.42-10.01 & \\ 7.21 & -0.18 & -7.04 & 0.96 & -10.01 & 48.22 \end{pmatrix} \text{GPa},$$

This has the characteristics of a generally anisotropic solid, thereby serving to demonstrate the capability of the algorithm to treat such solids. To verify the results obtained, the problem is also analyzed using the commercial finite element method (FEM) code, ANSYS. The mesh designs employed in BEM and FEM are shown in Fig. 3(b) and (c), respectively. Table 2 lists the results obtained using the two techniques. It can be seen that they are, again, in very good agreement.

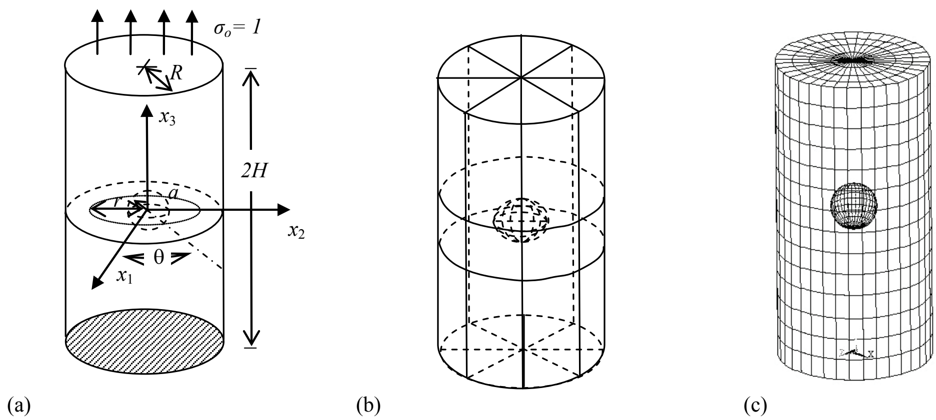

Figure 2: (a) A cylinder with a spherical cavity under remote tension - *Example (B)*; (b) BEM mesh employed – 88 quadratic elements, 228 nodes; (c) FEM mesh employed with ANSYS – 2940 SOLID186 elements with 6826 nodes.

Table 2: Resultant displacements and normalized von Mises equivalent stress, σ_{eq}/σ_o, at points on the plane of the equator of the spherical cavity- *Example (B)*.

	$\delta = \sqrt{u_1^2+u_2^2+u_3^2}(*10^{-9})$			σ_{eq}/σ_o		
θ	FEM	BEM	|%Diff.|	FEM	BEM	|%Diff.|
0^0	0.1104	0.1078	2.39	1.1268	1.1218	0.44
45^0	0.1236	0.1209	2.16	1.1168	1.1080	0.79
90^0	0.1362	0.1335	1.99	1.0919	1.0844	0.69
135^0	0.1381	0.1351	2.15	1.0799	1.0737	0.58
180^0	0.1203	0.1175	2.30	1.1192	1.1107	0.76
225^0	0.1040	0.1011	2.80	1.1172	1.1098	0.64
270^0	0.1033	0.1003	2.91	1.1054	1.0998	0.50
315^0	0.1064	0.1036	2.63	1.0824	1.0781	0.39

4 Conclusions

Following an approach suggested by Lee (2009) very recently, first- and second-order derivatives of the Green's function for a 3D generally anisotropic solid have been successfully derived in fully explicit, algebraic forms in terms of Stroh's eigenvalues. This has enabled the numerical implementation of Somigliana's identities for obtaining displacements and stresses at interior points of an anisotropic solid in BEM, in the same vein as has been well established in isotropic elasticity. It has never been previously achieved in the literature using other forms of the Green's function because of the mathematical complexity. In addition, there are no very high order tensor quantities being introduced that may incur disproportionate computing effort to evaluate. Two example problems have been presented to demonstrate the veracity and successful implementation of the formulations derived.

Acknowledgement: The work described in this paper is supported by research grants received by the authors from the National Science & Engineering Research Council of Canada and the National Science Council of Taiwan, ROC (NSC 99-2221-E-035-MY3), respectively.

References

Huntington, H.B. (1968): *The Elastic Constants of Crystals.* Academic Press, New York.

Lifshitz, I.M., Rozenzweig, L.N. (1947): On the construction of the Green tensor for the basic equation of the theory of elasticity of an anisotropic infinite medium. *Zh. Eksp. Teor. Fiz.*, **17**, 783-791.

Lee, V.G. (2003): Explicit expression of derivatives of elastic Green's functions for general anisotropic materials. *Mech. Res. Comm.*, 30, 241–249.

Lee, V.G. (2009): Derivatives of the three-dimensional Green's function for anisotropic materials. *Int. J.Solids Struct.*, **46**, 3471-3479.

Lekhnitskii, S.G. (1963): *Theory of Elasticity of an Anisotropic Body*. Holden-Day Publishers, San Francisco.

Phan, P.V.; Gray, L.J.; Kaplan, T. (2004): On the residue calculus evaluation of the 3D anisotropic elastic Green's function. *Comm. Numer. Methods Engng.*, 20, 335-341.

Sales, M.A.; Gray, L.J. (1998): Evaluation of the anisotropic Green's function and its derivatives. *Comp. & Struct.*, 69,247-254.

Shiah, Y.C.; Tan, C.L.; Lee, V.G.; Chen, Y.H. (2008): Evaluation of Green's functions for 3D anisotropic elastic solids. *Advances in Boundary Element Techniques IX*, *Proc. BeTeq 2008 Conf.*, *Seville*, R. Abascal & M.H. Aliabadi (eds.), E.C. Ltd. (U.K.), 119-124.

Shiah, Y.C.; Tan, C.L.; Lee, R.F. (2011): Internal point solutions or displacements and stresses in 3D anisotropic elastic solids using the boundary element method. *CMES* (*submitted Dec. 2010*).

Tan, C.L., Shiah, Y.C. and Lin, C.W. (2009): Stress analysis of 3D generally anisotropic elastic solids using the boundary element method. *CMES,* **41**, 195-214.

Ting, T.C.T.: Lee,V.G. (1997):The 3D elastostatic Green's function for general anisotropic linear elastic solid. *Q. J. Mech. Appl. Math.*, 50, 407-426.

Tonon, F.; Pan, E.; Amadei, B. (2001): Green's functions and boundary element method formulation for 3D anisotropic media. *Comp. & Struct.*, 79, 469-482.

Wang, C.Y.; Denda, M. (2007): 3D BEM for general anisotropic elasticity. *Int. J. Solids Struct.*, 44, 7073-7091.

Wilson, R.B.; Cruse, T.A. (1978): Efficient implementation of anisotropic three dimensional boundary integral equation stress analysis. *Int. J. Numer. Methods Engng.*, 12, 1383-1397.